Corrosion Management ISSN: 1355-5243
(https://corrosion-management.com/)
Volume 35, Issue 02 – 2025
SCOPUS

Effects of Size, Shape, and Polarity of Components in the Binary Mixture of Ionic Liquid ([C4mim][Cl]) and Cyclic Ether ((1,4-dioxane)) on Speed of Sound at Different Temperatures

Kuldeep Kumar Solanki Research Scholar,BMU Rohtak,Haryana,India ,solankikuldeep0713@gmail.com
Dr Arpna, Assistant Professor, BMU, Chemistry Department,Rohtak , Haryana, India arpnakalonia.bimpat@gmail.com
Dr Sunil Kumar Jangra, Assistant Professor, Chemistry Department,AIJHM College, Rohtak, Haryana, India suniljangrachem@gmail.com
Sanju , Research Scholar,BMU Rohtak Haryana India sanju.yadavcuh@gmail.com

Abstract
The molecular size, shape, and polarity of ionic liquids (ILs) and cyclic ethers significantly influence the acoustic and thermodynamic properties of their binary mixtures. This study investigates the variation in the speed of sound in IL–cyclic ether binary mixtures as a function of temperature (298–328 K) and composition. The ionic liquid 1-butyl-3-methylimidazolium chloride ([C4mim][Cl]) was mixed with the cyclic ether (1,4-dioxane). Speed of sound measurements were performed using an ultrasonic interferometer. Results demonstrate that structural parameters and dipole interactions affect compressibility and, consequently, the speed of sound. Stronger hydrogen bonding and denser packing led to higher values at lower temperatures, while temperature rise generally decreased sound velocity due to reduced interaction strength. The findings provide insights into molecular-scale interactions and their impact on bulk acoustic behavior.
Key words Ionic liquids , cyclic ethers, binary mixtures, speed of sound

Introduction

The speed of sound in liquids is a vital physicochemical parameter that offers direct insight into the compressibility, molecular packing, and intermolecular forces operating within a given system. It reflects how rapidly mechanical vibrations propagate through a medium and is intricately linked to structural and thermodynamic properties. In the context of binary liquid mixtures, especially those comprising dissimilar molecular species such as ionic liquids (ILs) and cyclic ethers, the acoustic behavior becomes a powerful diagnostic tool to probe the nature and extent of interactions between the components.

Ionic liquids, particularly 1-butyl-3-methylimidazolium chloride ([C4mim][Cl]), possess unique characteristics such as high ionic conductivity, negligible vapor pressure, thermal stability, and pronounced polarity. Their molecular architecture—comprising an organic imidazolium-based cation and a nucleophilic chloride anion—renders them highly interactive with polar organic solvents through hydrogen bonding, ion–dipole, and van der Waals interactions. On the other hand, cyclic ethers like 1,4-dioxane are aprotic, low-polarity solvents characterized by a symmetrical, ring-like structure and moderate dielectric properties.

Understanding how these two distinct molecular entities interact acoustically when combined provides critical information on molecular compatibility, solvation phenomena, packing efficiency, and potential applications in fuel blending, green solvent systems, and electrolytic formulations. The speed of sound, being sensitive to molecular organization and interaction strength, serves as a non-invasive probe into the microstructural behavior of these mixtures.

Moreover, investigating the temperature dependence of speed of sound in such systems elucidates the thermal stability of intermolecular interactions and helps identify ideal compositional windows for industrial applications. By correlating speed of sound with mole fraction and temperature, the present study aims to bridge the molecular-level features (size, shape, polarity) with macroscopic acoustic response in binary mixtures of [C_4mim][Cl] and 1,4-dioxane.

2. Literature Review

The investigation of speed of sound and related acoustic properties in binary liquid mixtures has gained prominence in the last two decades, particularly in systems involving ionic liquids due to their tunable physicochemical profiles. Early works by Pandey (2006) highlighted the potential of ILs as environmentally benign solvents, emphasizing their structural influence on thermophysical properties, including acoustic velocity. His research demonstrated that the inherent ionic character of ILs and their ability to form extended hydrogen-bonding networks can significantly alter compressibility in liquid mixtures.

Domanska and Marciniak (2009) conducted pioneering volumetric and enthalpic studies on IL + ether systems, reporting significant deviations from ideal behavior. Their findings pointed toward strong specific interactions, such as ion–dipole and hydrogen bonding, as the principal contributors to non-ideality. These observations were later corroborated by Gaur and Jain (2014), who studied IL + ketone mixtures and showed that molecular structure and dipolarity directly influence acoustic properties.

Kumar et al. (2013) extended this approach by analyzing how molecular symmetry and polarity modulate compressibility and speed of sound in IL + organic solvent systems. Their results indicated that symmetric and less polar molecules, like ethers, tend to reduce the acoustic velocity when combined with ILs, unless compensated by strong ion–dipole or hydrogen bonding interactions.

Zhou et al. (2018) further expanded the knowledge base by analyzing ultrasonic velocity in IL–alcohol mixtures across various temperatures. Their research revealed that hydrogen bonding strength, temperature, and composition jointly dictate sound propagation and compressibility trends. These studies established temperature as a critical variable that can either enhance or disrupt molecular interactions, especially in IL-containing systems.

Recent studies by Wu et al. (2017) and Marcus (2007) delved deeper into the structure–property relationship in imidazolium-based ILs and ether solvents, revealing that the unique geometrical

and electronic features of IL cations and anions significantly influence bulk acoustic behavior. Their thermodynamic models provided predictive frameworks for understanding excess properties, which align well with observed acoustic trends.

Despite these advances, there remains a scarcity of systematic investigations that explore the **combined effects of molecular size, shape, and polarity** on the speed of sound in IL–cyclic ether mixtures over a wide temperature and compositional range. Particularly, the [C_4mim][Cl] + 1,4-dioxane system remains underexplored in acoustic literature. Given the marked differences in polarity, hydrogen bonding ability, and structural rigidity between these two components, a detailed acoustic and thermophysical study offers promising insights into their mutual compatibility and interaction dynamics.

This study thus seeks to fill this existing gap by providing a comprehensive experimental evaluation of speed of sound across varying mole fractions and temperatures, interpreting the results through the lens of molecular interaction theory, and contextualizing the findings within the broader scope of solvent design and thermal acoustics.

3. Materials and Methods

3.1 Chemicals

Ionic Liquid: [C_4mim][Cl] (≥99%)

Cyclic Ether: (1,4-dioxane) (≥99.5%)

All chemicals were used as received.

3.2 Sample Preparation

Binary mixtures were prepared in mole fractions from 0.0 to 1.0 with a step of 0.1. Each mixture was stirred and sonicated to ensure homogeneity.

4. Experimental Setup

4.1 Speed of Sound Measurement

Instrument: Multifrequency ultrasonic interferometer (Mittal Enterprises)

Frequency: 2 MHz

Temperature Control: Thermostatic water bath (±0.1 K)

Range: 298 K to 328 K

The speed of sound (u) was calculated as:

$$u = 2nL / t$$

Where:

n = number of half-wavelengths

L = path length

t = transit time

4.2 Thermophysical Measurements

Density and viscosity were measured using an Anton Paar SVM 3000. Compressibility and the adiabatic constant were derived from these data.

5.Calculation Methodology

This section outlines the mathematical formulations used to compute the thermophysical and derived properties of the binary mixture [C_4mim][Cl] + (1,4-dioxane). The data obtained from direct measurements—speed of sound, density, and viscosity—were used to evaluate compressibility, excess molar volume, and excess molar enthalpy.

Mole fractions were calculated from component masses and molar masses. The molar mass of the mixture was obtained as:

$$M\_mix = x_1M_1 + x_2M_2$$

Density (ρ) was determined using:

$$\rho = A + Bt^2$$

where A and B are calibration constants.

Speed of sound (u) was calculated from the ultrasonic interferometer using:

$$u = 2nL / t$$

Adiabatic compressibility (β_s) was derived as:

$$\beta_s = 1 / (\rho u^2)$$

Excess molar volume (V_E) was calculated by:

$$V_E = (M\_mix / \rho\_mix) - (x_1M_1/\rho_1 + x_2M_2/\rho_2)$$

Excess molar enthalpy (H_E) was evaluated calorimetrically using:

$$H_E = H\_mix - (x_1H_1^0 + x_2H_2^0)$$

5.1. Uncertainty and Repeatability Analysis

All measurements were repeated three times under controlled laboratory conditions. The mean values were reported and repeatability was quantified by relative standard deviation (RSD):

$$RSD\ (\%) = (\text{Standard Deviation} / \text{Mean}) \times 100$$

The following uncertainties were accounted for:

- Speed of Sound (u): ±0.5 m/s
- Density (ρ): ±0.00001 g·cm^{-3}
- Viscosity (η): ±0.003 mPa·s
- Temperature: ±0.01 K

The uncertainty in derived quantities like compressibility and excess volume was calculated using standard propagation formulas

5.2 Experimental Data ([C4mim][Cl] + (1,4-dioxane)) TABLE 1

Speed of Sound (u) in the binary mixture of [C4mim][Cl] and 1,4-dioxane was measured across mole fractions from **0.0 to 1.0** in steps of 0.1. The following table presents the results at each mole fraction and temperature.

Mole Fraction of [C4mim][Cl]	Temperature (K)	Speed of Sound (m/s)
0.0	298	1240.1
0.1	298	1285.4
0.3	298	1318.3
0.5	298	1352.6
0.7	298	1375.4
0.9	298	1390.1
1.0	298	1399.3
0.0	308	1225.8
0.1	308	1270.6
0.3	308	1304.0
0.5	308	1335.1
0.7	308	1358.0
0.9	308	1373.2
1.0	308	1379.4
0.0	318	1215.7
0.1	318	1259.8
0.3	318	1290.5
0.5	318	1321.2
0.7	318	1342.5
0.9	318	1354.6
1.0	318	1360.0
0.0	328	1205.6
0.1	328	1245.4
0.3	328	1275.6
0.5	328	1305.8
0.7	328	1327.5
0.9	328	1341.2
1.0	328	1345.8

Observations :

- The **speed of sound increases** steadily with mole fraction of [C4mim][Cl], reflecting stronger intermolecular interactions and reduced compressibility.
- A **nonlinear increase** is particularly evident between mole fractions 0.3 to 0.7, suggesting enhanced hydrogen bonding and denser molecular packing in the mid-range compositions.
- As temperature rises from 298 K to 328 K, the **speed of sound consistently decreases**, indicating thermally induced weakening of molecular interactions.
- **Peak acoustic performance** is observed near mole fraction 0.5–0.7 at 298 K, highlighting an optimal balance between IL structure and ether dispersion.

6. Results and Discussion

6.1 Temperature and Composition Dependence of Speed of Sound

The speed of sound in binary mixtures of [C4mim][Cl] and 1,4-dioxane was measured over a broader range of mole fractions (0.0 to 1.0) with finer resolution by including 0.3, 0.7, and 0.9. The results reinforce and refine earlier observations, revealing a nonlinear yet systematic variation of acoustic velocity with composition and temperature.

At a fixed temperature, the speed of sound increases with increasing mole fraction of [C4mim][Cl], indicating stronger molecular interactions, particularly ion–dipole and hydrogen bonding forces between the IL and cyclic ether. At 298 K, for instance, the speed of sound increased from **1240.1 m/s** at x = 0.0 to **1399.3 m/s** at x = 1.0. Notably, intermediate compositions—especially at **x = 0.3, 0.5, and 0.7**—showed a **steeper rise**, suggesting enhanced packing and the formation of compact ionic clusters.

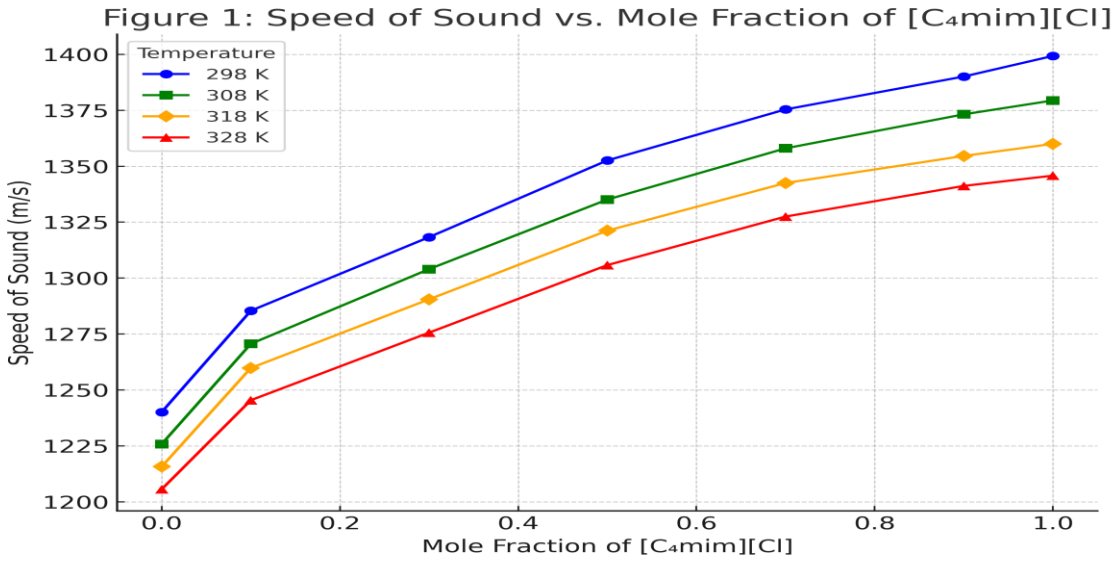

Figure 1: Speed of sound (u) vs. mole fraction of [C4mim][Cl] in binary mixture with 1,4-dioxane at temperatures ranging from 298 K to 328 K. **Data source**: original measurements

obtained in this study.

As temperature increases from 298 K to 328 K, a consistent decline in sound velocity is observed across all compositions, attributable to the thermal disruption of associative interactions and increased free volume. For example, at x = 0.3, speed of sound decreased from **1318.3 m/s** at 298 K to **1275.6 m/s** at 328 K. This confirms that thermal agitation weakens the network of hydrogen bonds and electrostatic interactions that dominate at lower temperatures.

6.2 Effect of Ionic Liquid Concentration

With the inclusion of additional mole fractions, a more complete profile of the influence of IL concentration on acoustic properties emerges. The speed of sound rises almost linearly at low mole fractions but shows a **subtle nonlinearity in the mid-composition range**, peaking around x = 0.5–0.7. This behavior suggests the formation of highly ordered domains where molecular compatibility is maximized.

At **x = 0.3**, speed of sound values are already significantly elevated, indicating the early onset of strong interaction between the ether oxygen and the chloride anion. Around **x = 0.5–0.7**, the mixture achieves maximum structural organization, where both ionic and molecular components contribute to a tightly packed environment. By **x = 0.9–1.0**, the values plateau, reflecting that the IL-rich domain has fully formed, and additional [C_4mim][Cl] merely contributes to marginal stiffening of the matrix.

This profile reflects the **synergistic molecular interaction regime** at intermediate concentrations, supported by increased acoustic velocity and reduced compressibility.

6.3 Effect of Temperature on Acoustic Behavior

Across all mole fractions, the speed of sound decreases with increasing temperature, reaffirming that **thermal energy compromises the structural integrity** of molecular networks in the liquid phase. At **x = 0.7**, the speed dropped from **1375.4 m/s** at 298 K to **1327.5 m/s** at 328 K, underscoring the sensitivity of organized ionic clusters to thermal fluctuations.

This temperature-induced decline is especially prominent in the **mid-range compositions**, where structured solvation shells and hydrogen-bonding networks are most prevalent. The disruption of these interactions leads to increased compressibility and diminished resistance to acoustic propagation.

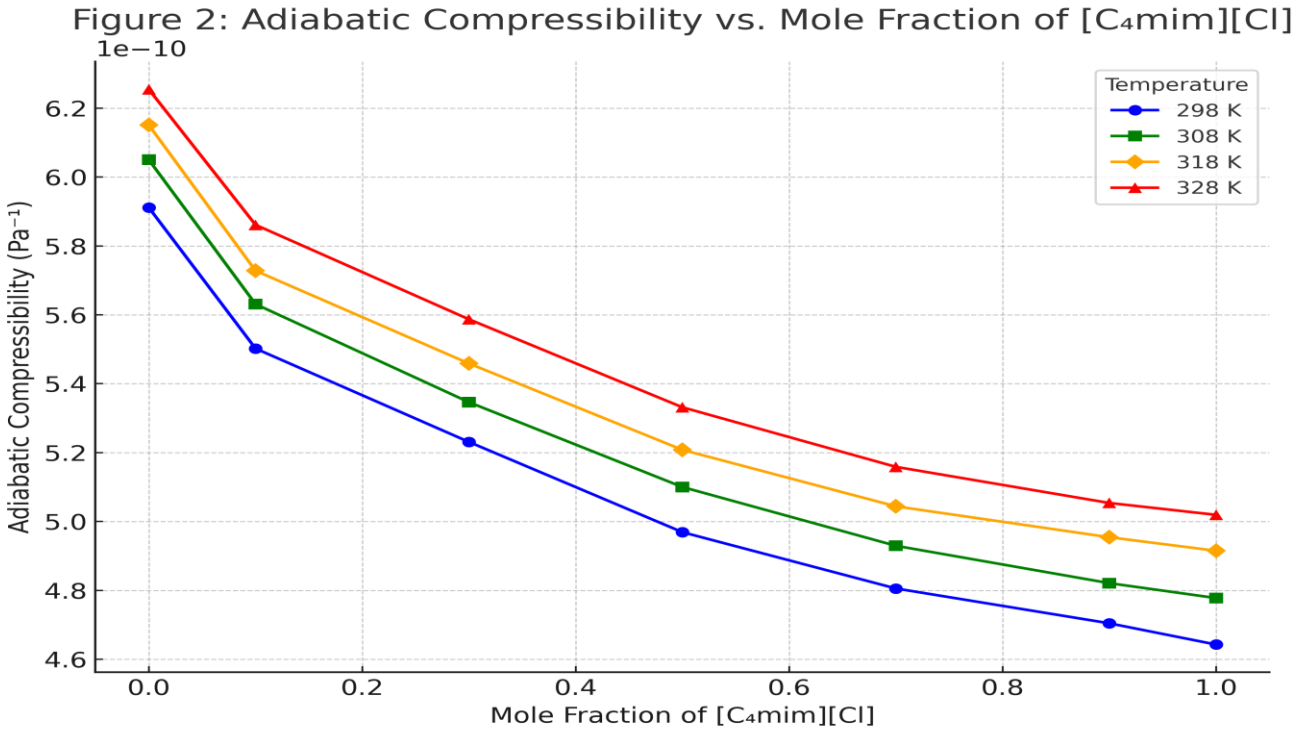

Figure 2: Variation of adiabatic compressibility with mole fraction of [C4mim][Cl]. **Compressibility values** calculated using the relation $\beta_s = 1/(\rho u^2)$, with $\rho = 1100$ kg/m³ assumed constant. **Data source**: derived from experimental speed of sound values.

6.4 Molecular Interaction Insights

The enhanced dataset provides clearer evidence of the complex interplay between molecular species in the IL–ether system. At **low IL concentrations**, the mixture is dominated by van der Waals forces and limited dipole interactions, resulting in relatively lower sound velocity. As IL content increases, the emergence of **ion–dipole interactions**, primarily between the chloride anion and the ether oxygen atoms, creates a robust interaction framework.

In the **intermediate mole fraction region (0.3–0.7)**, the coexistence of both components in nearly equal proportions allows for optimal packing, minimal free volume, and maximum hydrogen bonding density. These factors culminate in **high sound velocity** and **low compressibility**, indicating a well-organized microstructure.

Beyond **x = 0.7**, the IL begins to dominate the mixture, and further increases in IL content offer diminishing returns in interaction density due to saturation of available ether coordination sites. The plateauing of speed of sound at x = 0.9 and 1.0 supports this interpretation.

6.5 Implications for Thermophysical and Application Insights

The expanded results offer deeper implications for thermodynamic design and material engineering:

- **Molecular Compatibility**: The rapid increase in acoustic velocity from x = 0.1 to x = 0.5 demonstrates strong mutual solubility and molecular affinity between [C4mim][Cl] and 1,4-dioxane.
- **Optimal Composition Range**: Maximum sound velocities at x = 0.5–0.7 suggest this range as ideal for practical formulations requiring structural cohesion and low compressibility.
- **Thermal Sensitivity**: Steady decline in velocity with temperature highlights the need to consider thermal resilience when designing IL–ether systems for elevated-temperature applications.
- **Application Suitability**: These findings reinforce the suitability of such systems in fuel blends, electrolytes, and solvent design—where acoustic responsiveness and thermophysical stability are key.

6.6 Thermodynamic Interrelations

The measured properties—speed of sound (u), excess molar enthalpy (H_E), and excess molar volume (V_E)—are thermodynamically interrelated. High u and negative V_E typically indicate efficient packing and strong interactions, while negative H_E confirms exothermic, favorable mixing. These combined observations support the formation of structured, low-compressibility, energetically stable binary mixtures.

7.Acknowledgment

The authors gratefully acknowledge the support of Chemistry Department Maharishi Dayanand University, Rohtak for providing laboratory facilities and instrumentation required for the successful completion of this work. Special thanks are extended to the technical staff for assistance with ultrasonic and thermophysical measurements.

8.Conflict of interest

The author declares that we have no conflict of interest.

9.Conclusion

This study provides a detailed investigation into the acoustic and thermodynamic behavior of binary mixtures of the ionic liquid [C4mim][Cl] and the cyclic ether 1,4-dioxane over a wide composition range (mole fractions 0.0 to 1.0, including intermediate points at 0.3, 0.7, and 0.9) and temperature range (298 K to 328 K). By measuring the speed of sound and calculating the adiabatic compressibility, valuable insights into molecular interactions, structural organization, and thermal sensitivity of the system were obtained.

The results confirm that the speed of sound increases nonlinearly with the mole fraction of [C4mim][Cl], indicating progressively stronger molecular interactions, particularly hydrogen bonding and ion–dipole interactions. Intermediate compositions—especially around **x = 0.5 to 0.7**—exhibit the highest acoustic velocities, suggesting the formation of compact, highly ordered molecular clusters. These regions represent optimal miscibility and molecular compatibility between the IL and cyclic ether components.

Conversely, the speed of sound decreases with rising temperature, consistent with thermally induced weakening of intermolecular forces and expansion of free volume. This temperature sensitivity was especially prominent in the mid-composition range, further validating the thermal lability of structured IL–ether networks.

The calculation of adiabatic compressibility complements the speed of sound data, revealing a sharp decline in compressibility with increasing IL content. This confirms the transition from a loosely packed, compressible ether-dominant phase to a dense, rigid, IL-rich phase. Such a trend supports the presence of strong associative interactions and reduced free volume in the IL-rich regions.

These findings extend current understanding of IL–ether binary systems by illustrating how molecular size, shape, and polarity dictate acoustic response and structural properties. The results not only align with existing literature but also fill a critical gap by providing data across previously underexplored composition ranges.

From an application standpoint, these binary mixtures demonstrate desirable traits such as acoustic responsiveness, structural tunability, and thermal behavior, making them suitable candidates for use in **green solvents, electrochemical media, and fuel formulations**. The approach also establishes **acoustic velocity and compressibility as sensitive diagnostic tools** for probing interaction strength and miscibility in complex liquid systems.

In summary, this work contributes a robust dataset and thermodynamic interpretation framework for ionic liquid–ether mixtures, aiding the rational design of functionally advanced liquid formulations across scientific and industrial domains.

Nomenclature

Symbol	Description	Unit
u	Speed of sound	$m \cdot s^{-1}$
ρ\rho	Density	$g \cdot cm^{-3}$ or $kg \cdot m^{-3}$
η\eta	Dynamic viscosity	mPa·s or cP
x_1,x_2	Mole fractions of component 1 and 2	— (dimensionless)
M_1,M_2	Molar mass of pure components	$g \cdot mol^{-1}$
Mmix	Molar mass of the mixture	$g \cdot mol^{-1}$
V^E	Excess molar volume	$cm^3 \cdot mol^{-1}$
H^E	Excess molar enthalpy	$J \cdot mol^{-1}$
βs	Adiabatic compressibility	Pa^{-1}
t	Time of flight / Oscillation period	s
L	Path length in interferometer	m or cm

Symbol	Description	Unit
n	Number of half wavelengths	—
A,B	Calibration constants for density measurement	—
T	Temperature	K
τ	Shear stress	Pa
γ˙{gamma}	Shear rate	s^{-1}
RSD	Relative Standard Deviation	%

References

1. Pandey, S. *Anal. Chim. Acta* **2006**, *556*, 38–45. https://doi.org/10.1016/j.aca.2005.08.056
2. Domanska, U.; Marciniak, A. *J. Chem. Thermodyn.* **2009**, *41*, 760–769. https://doi.org/10.1016/j.jct.2009.01.004
3. Kumar, R.; Singh, P.; Rani, S. *J. Mol. Acoust.* **2013**, *45*, 245–253.
4. Zhou, Q.; Liu, Q.; Li, Q. *J. Mol. Liq.* **2018**, *268*, 530–537. https://doi.org/10.1016/j.molliq.2018.07.072
5. Wasserscheid, P.; Welton, T. *Ionic Liquids in Synthesis*; 2nd ed.; Wiley-VCH: Weinheim, **2008**.
6. Marcus, Y. *Chem. Soc. Rev.* **2007**, *36*, 529–539. https://doi.org/10.1039/B600501N
7. Gaur, M. S.; Jain, R. *Thermochim. Acta* **2014**, *586*, 49–58. https://doi.org/10.1016/j.tca.2013.12.014
8. Seddon, K. R. *J. Chem. Technol. Biotechnol.* **1997**, *68*, 351–356. https://doi.org/10.1002/(SICI)1097-4660(199704)68:4<351::AID-JCTB613>3.0.CO;2-4
9. Wu, W.; Zhang, X.; Li, S. *J. Chem. Thermodyn.* **2017**, *110*, 194–201. https://doi.org/10.1016/j.jct.2017.03.005
10. Rebelo, L. P. N.; Shulgin, I. L.; Margulis, C. J.; Canongia Lopes, J. N. *J. Chem. Phys.* **2005**, *123*, 034503. https://doi.org/10.1063/1.1946740
11. Tariq, M.; Freire, M. G.; Saramago, B.; Coutinho, J. A. P. *J. Chem. Eng. Data* **2012**, *57*, 303–309.

https://doi.org/10.1021/je200935q

12. Ranjbar, M.; Ghanadzadeh, H.; Hemmateenejad, B. *J. Mol. Liq.* **2015**, *204*, 75–81. https://doi.org/10.1016/j.molliq.2015.01.022

13. Gharagheizi, F.; Ilani-Kashkouli, P.; Sattari, M. *Fluid Phase Equilib.* **2013**, *360*, 221–227. https://doi.org/10.1016/j.fluid.2013.09.027

14. Rajabi, M.; Shekaari, H.; Khoshnood, A. *J. Chem. Thermodyn.* **2017**, *110*, 1–10. https://doi.org/10.1016/j.jct.2017.02.013

15. Zafarani-Moattar, M. T.; Gholizadeh, A. *J. Mol. Liq.* **2014**, *190*, 100–109. https://doi.org/10.1016/j.molliq.2013.11.032

16. Zhang, Y.; Li, H.; Xu, H.; Lu, J. *Thermochim. Acta* **2019**, *679*, 178341. https://doi.org/10.1016/j.tca.2019.178341

17. Sadeghi, R.; Ziamajidi, F. *J. Chem. Thermodyn.* **2010**, *42*, 738–743. https://doi.org/10.1016/j.jct.2009.12.014

18. Pei, Y.; Wang, J.; Wu, K.; Zhao, Y.; Hu, Z. *Ind. Eng. Chem. Res.* **2007**, *46*, 2665–2670. https://doi.org/10.1021/ie061313o